Quantum mechanical interference in the photorecombination of highly charged mercury ions

A. J. González Martínez [a], A. Artemyev [b], J. Braun [a], G. Brenner [a], H. Bruhns [a], J. R. Crespo López-Urrutia [a], A. Lapierre [a], V. Mironov [a], J. Scofield [c], R. Soria Orts [a], H. Tawara [a], M. Trinczek [a], I. Tupytsin [b], J. Ullrich [a]

[a] *Max-Planck Institute for Nuclear Physics, D-69117 Heidelberg, Germany*
[b] *St. Petersburg State University, St. Petersburg 198504, Russia*
[c] *Lawrence Livermore National Laboratory, Livermore, CA 94550, USA*

Abstract

We present preliminary experimental data on the quantum interference between the direct and dielectronic recombination of highly charged mercury ($Hg^{75+...78+}$) ions in an EBIT. The Fano factors which characterize the asymmetry level as well as absolute excitation energies have been measured and compared with theoretical calculations. The high resolution achieved in the present experiment (10^{-4}) allows us to isolate blended resonances. In addition, the fine structure splitting between levels with different total angular momentum J was determined with uncertainties as low as 3 eV for the ion charge states present in the experiment.

Key words: Quantum interference; X-ray spectroscopy; EBIT; QED
PACS: 34.80.Kw, 32.80.Hd, 52.25.Os

1. Introduction

Detailed studies of heavy highly charged ions (HCI) are needed to test quantum electrodynamics (QED) contribution in strong fields, and to obtain a better understanding of the electronic structure. In particular, the QED contributions are as large as 160 eV for the 1s electron in mercury (Z=80) ions with which the present work deals. Furthermore, the calculated energies for the 1s level of these few-electron systems are shifted due to finite nuclear size effects by approximately 50 eV.

Our present experiment was motivated by the possibility of observing interference [1,2] between transitions leading directly into the continuum and those having a discrete autoionizing intermediate state in the photoionization of atoms. We observe the interference of the time-reversed processes, namely the radiative (direct) recombination and dielectronic (indirect) recombination of heavy HCI collisions with free electrons. Such interference results in asymmetric resonance profiles characterized by the so-called Fano-factor. Our experiment confirms with improved accuracy an earlier observation carried out in the LLNL Super-EBIT by Knapp *et al.* [3].

In the radiative recombination (RR), a free electron is captured into a vacant state of an ion emit-

ting a photon (γ_{RR}), see RR in Fig. 1. The dielectronic recombination (DR) is a resonant process where a free electron is captured and simultaneously a bound electron is excited. Later, the doubly excited state can decay into the ground state in most of the cases emitting one or more photons (γ_{DR}).

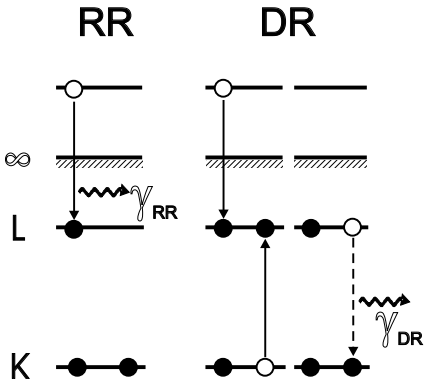

Fig. 1. Schematic representation of the direct (radiative) recombination (RR) in Li-like ions. The intermediate state formed via dielectronic recombination (DR) and the final state are shown.

The DR strength is defined as the product of the probability of the two steps needed for successful recombination, and therefore proportional to the capture probability into the doubly excited state and to the probability of such a state to decay radiatively to a non-autoionizing level. However, when the interacting electron energy is within the DR resonances, then it is not possible to know if the system has passed through the doubly excited state (DR) or if it went directly to the final state (RR). Both pathways are then indistinguishable and, therefore, quantum interference can occur. In order to experimentally observe a clear signature of interference, the two pathways must have similar intensities. This effect is enhanced in the KLL resonances of heavy HCI [4], where a free electron is captured into the L-shell while an electron in the K-shell is promoted to the L-shell. In the last decade a few theoretical approaches have been developed in order to consistently treat both processes in an unified way, see refs. [5–7].

The first clear sign of asymmetric resonance profiles in free-electron collisions with HCI was observed in the $KL_{1/2}L_{3/2}$ DR resonances of uranium

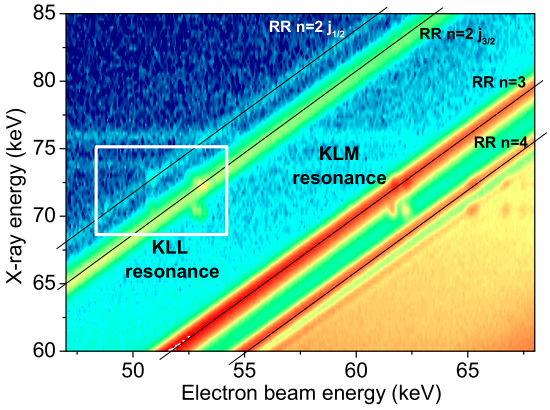

Fig. 2. Logarithmic 2D contour-plot of the recombination for highly charged mercury ions. The diagonal lines correspond to RR processes. DR processes are visible as bright spots. The enclosed rectangle shows the KLL region, whose projections onto the electron beam axis are shown in Fig. 3.

ions ($U^{87+...90+}$) [3]. However, they were averaged over all resonances corresponding to each one of the dominant ion charge states present in the trap. In the present experiment we observed similar resonance profiles in the whole KLL DR region of highly charged mercury ions ($Hg^{75+...78+}$). In contrast to the previous work, our improved resolution allows us to study the asymmetry as well as the absolute excitation energy for well-resolved resonances of different ion charge states.

2. Experimental setup

Mercury ions ranging from Hg^{75+} to Hg^{78+} were produced and trapped at the electron beam ion trap (EBIT) in Heidelberg [8,9]. Ionization takes place through successive collisions with an intense electron beam compressed with an 8 T magnetic field. Its negative space charge potential confines the ions in the radial direction. A set of independently biased electrodes, so-called drift tubes, are used to trap the ions longitudinally. The present experiment was carried out at an electron beam current of 160 mA. At first, the electron beam energy was slowly scanned over the range of 48 to 72 keV in a saw-tooth profile, and then in more detail over the KLL resonance region. A high-purity Ge-

detector mounted at 90 degrees relative to electron beam axis was used for the photon detection. The DR and RR processes are monitored through the emitted x-ray photons as a function of the electron beam energy. The electron energy is determined by measuring the acceleration voltage by means of two high-precision voltage dividers and correcting for space charge effects. The photon and the electron beam energies are simultaneously registered event by event and displayed in a two-dimensional plot, as shown in Fig. 2. Several diagonal bands due to RR process are clearly visible: from the top to the bottom, the upper band represents RR into n=2 states with the total angular momentum J=1/2, and the lower and broader band into those with J=3/2. The next two bands represent RR into the n=3 and n=4 states. The DR resonances are clearly distinguishable as isolated brighter spots. In the present work we have concentrated our analysis in the KLL DR region enclosed in a rectangle (Fig. 2). This region was scanned with higher resolution. Better statistics were also obtained.

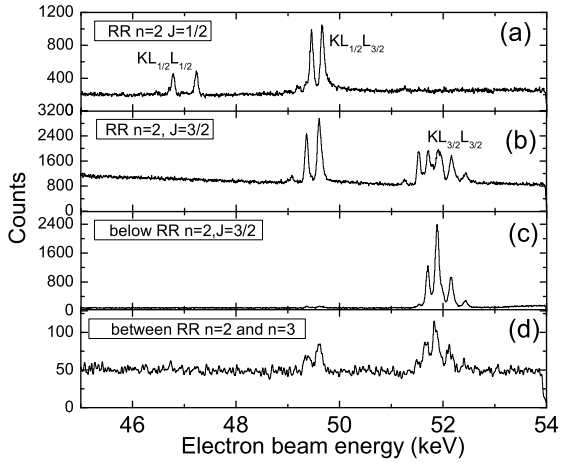

Fig. 3. a) Projection of the RR n=2, J=1/2 band where the $KL_{1/2}L_{1/2}$ and $KL_{1/2}L_{3/2}$ DR resonances are observed. b) Projection of the RR n=2, J=3/2 band which shows the $KL_{3/2}L_{3/2}$ DR resonances at higher electron energies. c) Projection below the RR n=2 bands. d) Projection of the two-photon transitions.

3. Data analysis

Four parallel regions have been projected onto the electron beam energy axis, see Fig. 3. The first projection (a) shows the RR n=2, J=1/2 band. It shows an overlap with the $KL_{J=1/2}L_{J=1/2}$ DR resonances and with the $KL_{J=1/2}L_{J=3/2}$ resonances at higher beam energies. The next projection at lower x-ray energies (b) shows the RR band into n=2, J=3/2. This cut overlaps with the $KL_{J=3/2}L_{J=3/2}$ DR region. The third (c) and fourth (d) cuts were performed in order to test our data acquisition and data analysis. The third projection (c), below the RR n=2 bands, passes through a set of DR resonances which do not overlap with the RR bands. The fourth one was performed also parallel to the previous cuts in between the RR n=2 band and n=3 and showed intense continuous distributions characteristic of two-photon transitions. Both the isolated resonances in the third projection and the observed peaks in the fourth one showed symmetric profiles, as expected, since no interference can happen in these two cases.

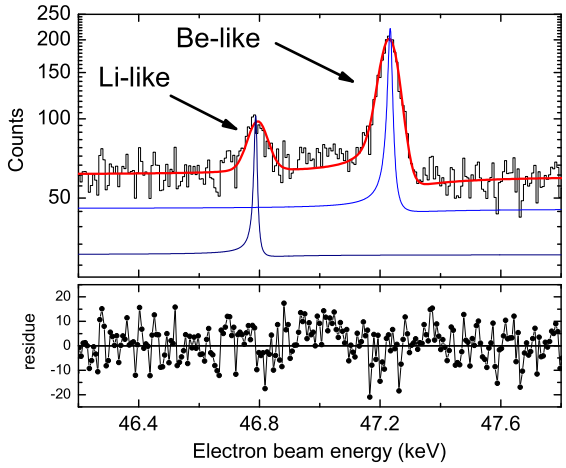

Fig. 4. Projection onto the electron beam energy axis of one of the thin cuts performed in the RR n=2, J=1/2 band. A little amount of Li-like ions is observed dominated by its next charge state of Be-like ions. The theoretical cross section (blue lines) normalized to the experimental data shows an enhanced asymmetry which tends to decrease when convoluted with the electron beam energy profile (red line). The scattered points near the zero Y-axis represent the residue plot of the observed data from the fitted curve.

4. Results

By slicing the upper two main projections into thinner cuts we are able to analyze in greater detail the interference for a specific charge state ion, see Fig. 4. It should be noted that the calculated natural width in Be- and B-like ions (blue line in Fig. 4) is as broad as 35 eV, comparable with the electron beam spread (≈50 eV). Therefore, our Fano-like function was convoluted with a normalized Gaussian distribution in order to fit the resonance profiles. The fit quality was tested with the χ^2 over degrees-of-freedom (DoF) method. A pure symmetric Lorentzian fit was also tried. Clearly, the convoluted Fano function always showed better agreement to the experimental data.

Table 1
Experimental data (in keV) for the fine structure splitting of C-like ions compared with two theoretical predictions, a multiconfiguration Dirac-Fock (MCDF) [10] and calculations performed in a QED framework (QED) with relativistic many body perturbation theory for the second order [11].

Excited states	**Experiment**	**MCDF**	**QED**
$KL_{3/2}L_{3/2}{}^a$ - $KL_{1/2}L_{3/2}{}^b$	2.047(7)	2.052	2.047
$KL_{3/2}L_{3/2}{}^a$ - $KL_{1/2}L_{3/2}{}^c$	2.104(7)	2.102	2.106
$KL_{1/2}L_{3/2}{}^b$ - $KL_{1/2}L_{3/2}{}^c$	0.057(3)	0.058	0.059

[a] $(1s2s^2 2p_{1/2})_{j_1=1}(2p_{3/2})^2{}_{j_2=2}$, J=3
[b] $1s2s^2(2p_{1/2})^2\ 2p_{3/2}$, J=1
[c] $1s2s^2(2p_{1/2})^2\ 2p_{3/2}$, J=2

The negative space charge potential, which reduces the electron beam energy, was estimated using standard formulae; at the current of 160 mA and 50 kV acceleration voltage it reduces the beam energy by roughly 100 eV. In this calculation we included a conservative estimate for the effect of positive space charge compensation due to the trapped ions. The estimate can be contrasted with the calculated excitation energies. We have compared the present result for the doubly excited state $1s\ 2s^2$ which is expected to have a symmetric resonance shape and the excitation energy of 46.358 keV. Our experimental value of 46.457(4) keV showed a space charge shift of 99(4) eV. With this shift and its corresponding scaling due to the electron beam energy, our experimental excitation energies can be determined with accuracies as low as 5 eV at 50 keV.

In addition to the absolute DR resonance energy, the fine structure splitting between states with different total angular momentum J for the observed resonances can also be accurately extracted. Such information is obtained through the differences between the experimental excitation energies, and shows a smaller experimental error. The measured fine structure splitting for the observed charge states agrees well with calculations [10,11]. As an example, Table 1 shows the experimental and theoretical results obtained from DR of Boron-like ions.

In future, dedicated measurements of the space charge potentials would allow to reduce the uncertainties of the absolute energy scale.

References

[1] U. Fano, Phys. Rev. **124**, 1866 (1961).

[2] U. Fano and J. W. Cooper, Phys. Rev. **137**, A1364 (1965).

[3] D. A. Knapp, P. Beiersdorfer, M. H. Chen, J. H. Scofield, and D. Schneider, Phys. Rev. Lett. **74**, 54 (1995).

[4] M. S. Pindzola, N. R. Badnell, and D. C. Griffin, Phys. Rev. A **46**, 5725 (1992).

[5] N. R. Badnell and M. S. Pindzola, Phys. Rev. A **45**, 2820 (1992).

[6] T. W. Gorczyca, M. S. Pindzola, F. Robicheaus, and N. R. Badnell, Phys. Rev. A **56**, 4742 (1997).

[7] V. L. Jacobs, J. Cooper and S. L. Haan, Phys. Rev. A **36**, 1093 (1987).

[8] J. R. Crespo López-Urrutia, A. Dorn, R. Moshammer, and J. Ullrich, Phys. Scr. **T80**, 502 (1999).

[9] J. R. Crespo López-Urrutia, B. Bapat, I. Draganic, A. Werdich, and J. Ullrich, Phys. Scr. **T92**, 110 (2001).

[10] J. Scofield, Phys. Rev. A **40**, 3054 (1989)

[11] A. Artemyev, V. M. Shabaev, M. M. Sysak, V. A. Yerokhin, T. Beier, G. Plunien and G. Soff, Phys. Rev. A **67**, 062506 (2003)